The Tumor Suppressor p53 Limits Ferroptosis by Blocking DPP4 Activity

Yangchun Xie, Shan Zhu, Xinxin Song, Xiaofang Sun, Yong Fan, Jinbao Liu, Meizuo Zhong, Hua Yuan, Lin Zhang, Timothy R. Billiar, et al.

Article

Cell Reports

The Tumor Suppressor p53 Limits Ferroptosis by Blocking DPP4 Activity

Graphical Abstract

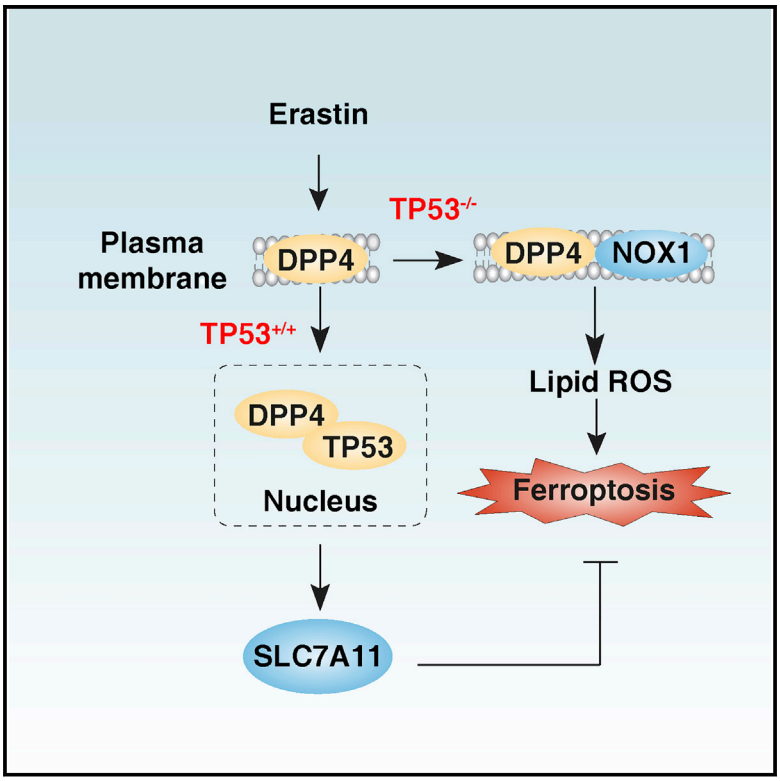

Authors

Yangchun Xie, Shan Zhu, Xinxin Song, ..., Rui Kang, Guido Kroemer, Daolin Tang

Correspondence

kroemer@orange.fr (G.K.), tangd2@upmc.edu (D.T.)

In Brief

Xie et al. find that TP53 antagonizes ferroptosis in colorectal cancer (CRC) cells by favoring the localization of DPP4 toward a nuclear, enzymatically inactive pool. This pathway is different from the previously identified function of TP53 as a positive regulator of ferroptosis in non-CRC cells.

Highlights

- TP53 inhibits ferroptosis in human colorectal cancer (CRC) cells
- TP53 mediates SLC7A11C expression in human CRC cells
- DPP4 mediates ferroptosis in TP53-deficient CRC cells
- Loss of TP53 enhances the anticancer activity of erastin *in vivo*

Xie et al., 2017, Cell Reports *20*, 1692–1704
August 15, 2017
http://dx.doi.org/10.1016/j.celrep.2017.07.055

OPEN ACCESS
CellPress

Cell Reports
Article

The Tumor Suppressor p53 Limits Ferroptosis by Blocking DPP4 Activity

Yangchun Xie,[1,2,3] Shan Zhu,[1] Xinxin Song,[3] Xiaofang Sun,[1] Yong Fan,[1] Jinbao Liu,[1] Meizuo Zhong,[2] Hua Yuan,[4] Lin Zhang,[5] Timothy R. Billiar,[3] Michael T. Lotze,[3] Herbert J. Zeh III,[3] Rui Kang,[3] Guido Kroemer,[6,7,8,9,10,11,12,*] and Daolin Tang[1,3,13,*]

[1]The Third Affiliated Hospital, Center for DAMP Biology, Key Laboratory for Major Obstetric Diseases of Guangdong Province, Key Laboratory of Reproduction and Genetics of Guangdong Higher Education Institutes, Protein Modification and Degradation Laboratory, Guangzhou Medical University, Guangzhou, Guangdong 510510, China
[2]Department of Oncology, Xiangya Hospital, Central South University, Changsha, Hunan 410008, China
[3]Department of Surgery, University of Pittsburgh, Pittsburgh, PA 15213, USA
[4]School of Nursing, Jilin University, Changchun, Jilin 130021, China
[5]Department of Pharmacology and Chemical Biology, University of Pittsburgh, Pittsburgh, PA 15213, USA
[6]Université Paris Descartes, Sorbonne Paris Cité, 75006 Paris, France
[7]Equipe 11 labellisée Ligue Nationale contre le Cancer, Centre de Recherche des Cordeliers, 75006 Paris, France
[8]Institut National de la Santé et de la Recherche Médicale, U1138, Paris, France
[9]Université Pierre et Marie Curie, 75006 Paris, France
[10]Metabolomics and Cell Biology Platforms, Gustave Roussy Cancer Campus, 94800 Villejuif, France
[11]Pôle de Biologie, Hôpital Européen Georges Pompidou, AP-HP, 75015 Paris, France
[12]Department of Women's and Children's Health, Karolinska University Hospital, 17176 Stockholm, Sweden
[13]Lead Contact
*Correspondence: kroemer@orange.fr (G.K.), tangd2@upmc.edu (D.T.)
http://dx.doi.org/10.1016/j.celrep.2017.07.055

SUMMARY

Ferroptosis is a form of regulated cell death that may facilitate the selective elimination of tumor cells. The tumor suppressor p53 (TP53) has been demonstrated to promote ferroptosis via a transcription-dependent mechanism. Here, we show that TP53 limits erastin-induced ferroptosis by blocking dipeptidyl-peptidase-4 (DPP4) activity in a transcription-independent manner. Loss of TP53 prevents nuclear accumulation of DPP4 and thus facilitates plasma-membrane-associated DPP4-dependent lipid peroxidation, which finally results in ferroptosis. These findings reveal a direct molecular link between TP53 and DPP4 in the control of lipid metabolism and may provide a precision medicine strategy for the treatment of colorectal cancer by induction of ferroptosis.

INTRODUCTION

The tumor suppressor p53 (TP53) is an evolutionarily conserved protein that plays essential roles in regulating cell proliferation, death, differentiation, and metabolism. While wild-type TP53 is normally a rapidly degraded protein, mutant forms of TP53 are stabilized and accumulate to high levels in tumor cells (Muller and Vousden, 2013). TP53 is stimulated by various external or internal stresses and is often described as the "guardian of the genome." For a long time, the tumor suppressor activity of TP53 was attributed to its capacity to initiate cell-cycle arrest and apoptosis under different stress stimuli through transcriptional and transcription-independent mechanisms (Bieging et al., 2014; Green and Kroemer, 2009; Khoo et al., 2014). Recent studies have suggested surprising roles for TP53 in tumor suppression independent of cell-cycle arrest and apoptosis (Li et al., 2012). In particular, induction of ferroptosis (an iron-dependent form of non-apoptotic cell death) as an additional mechanism may contribute to the oncosuppressive functions of TP53 (Jennis et al., 2016; Jiang et al., 2015; Wang et al., 2016b), indicating that TP53 may serve context-dependent functions in different types of regulated cell death.

Ferroptosis is a recently identified regulated type of death in cancer cells with oncogenic RAS mutations (Dixon et al., 2012). Unlike apoptosis and necroptosis, ferroptosis does not involve activation of caspase and mixed-lineage kinase-domain-like protein, respectively (Dixon et al., 2012; Yang et al., 2014). In contrast, lipid peroxidation plays a central role in mediating ferroptosis (Xie et al., 2016; Yang and Stockwell, 2016). In particular, acetyl coenzyme A (acyl-CoA) synthetase long-chain family member 4 (ACSL4) is critical for lipid peroxidation in ferroptotic cell death due to catalyzing esterification of arachidonoyl or adrenoyl into phosphatidylethanolamines (Doll et al., 2017; Kagan et al., 2017; Yuan et al., 2016). Pharmacologic induction of ferroptosis by small molecules such as erastin, sulfasalazine (SAS), or sorafenib has emerged as a strategy for the treatment of a variety of cancers, especially kidney cancer (Yang et al., 2014), leukemia (Yang et al., 2014; Yu et al., 2015), hepatocellular carcinoma (Louandre et al., 2013; Louandre et al., 2015; Sun et al., 2016a, 2016b), and pancreatic cancer (Eling et al., 2015; Hou et al., 2016; Zhu et al., 2017). However, cancer cells can display an adaptive response to ferroptosis by increasing expression of antioxidant enzymes and molecules. Thus, uncovering the

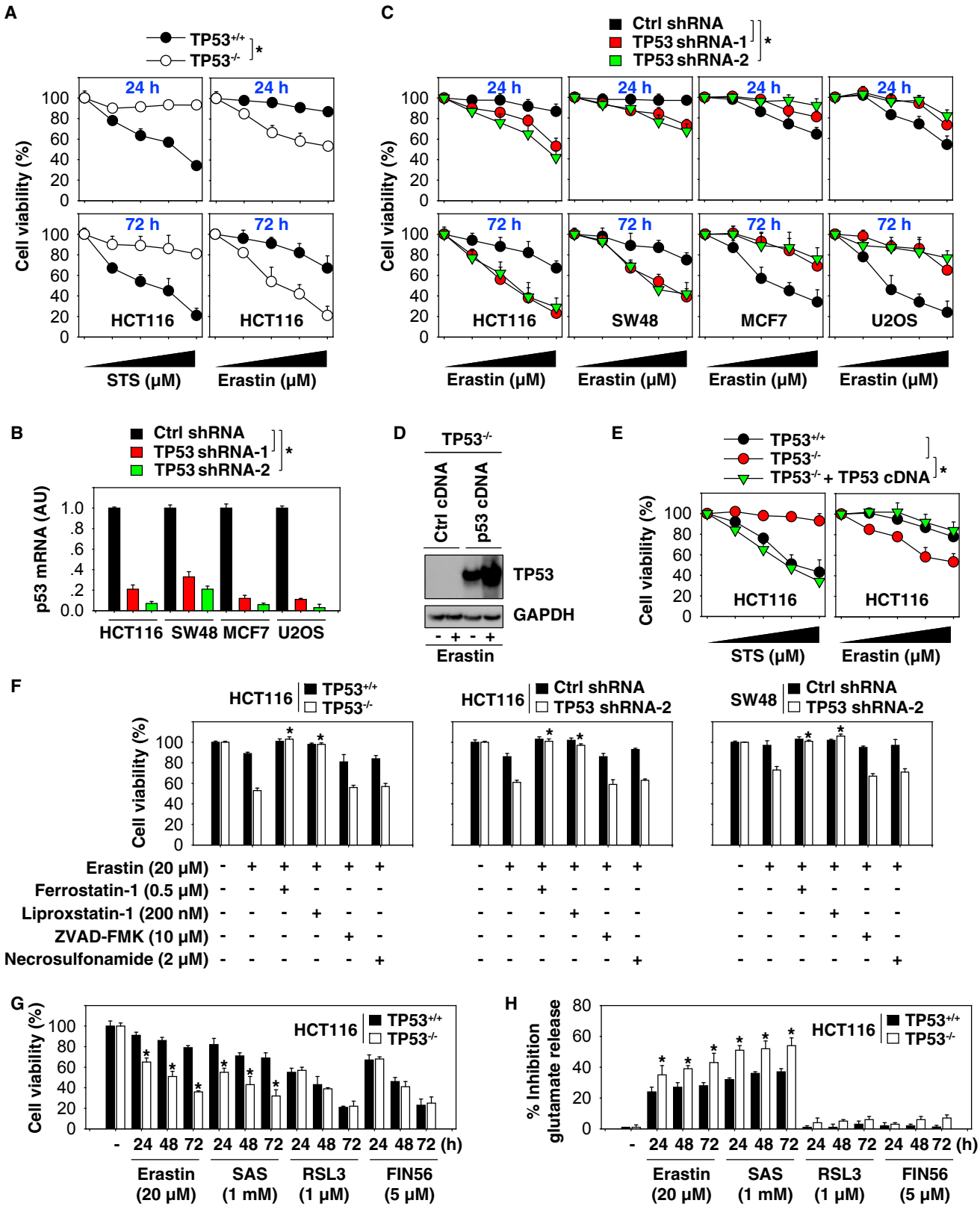

(legend on next page)

mechanism that promotes ferroptosis sensitivity versus resistance is critical for the development of personalized anti-cancer strategies.

Here, we demonstrate an unexpected role for TP53 in the regulation of erastin-induced ferroptosis in human colorectal cancer (CRC), the third most commonly diagnosed malignancy. Although TP53 promotes ferroptosis via a transcription-dependent mechanism in non-CRC cells, we report that TP53 inhibits ferroptosis by blocking dipeptidyl-peptidase-4 (DPP4) activity in a transcription-independent manner. These findings identify pleiotropic functions for TP53 in the regulation of ferroptosis and implicate DPP4 as a key coordinator of lipid metabolism within CRC.

RESULTS

TP53 Inhibits Ferroptosis in Human CRC Cells

K-RAS mutations can be found in 30%–50% of advanced-stage human CRC (Fearon, 2011). We therefore determined whether K-RAS mutations affect the anticancer activity of erastin in human CRC cell lines (e.g., HCT116 and SW48). Heterozygous knockin of K-RAS with an activating mutation at residue G12 in SW48 cells (Figure S1A) or depletion of K-RAS mutation at G13 in HCT116 cells (Figure S1B) did not affect the cell death induced by erastin compared to parental cell lines. These results support the emerging notion that induction of ferroptotic cancer cell death by erastin occurs through both RAS-dependent and RAS-independent mechanisms (Xie et al., 2016). Thus, improving the precision of genotype selection in the regulation of ferroptosis in different types of cancer is important for successful cancer therapy.

TP53 is also frequently inactivated by mutation or deletion in advanced human CRC (Fearon, 2011). Interestingly, recent studies show that activation of TP53 by erastin promotes ferroptosis in non-CRC cells (Jiang et al., 2015). To determine whether TP53 plays a similar role in CRC cells, we first investigated the relationship between TP53 status and sensitivity to erastin in several human CRC cell lines. CRC cell lines harboring mutant TP53 (CACO2, DLD1, and SW837) were more sensitive to erastin-induced death than wild-type (WT) TP53 cells (HCT116 and SW48) (Figures S2A and S2B). Knockin of a TP53 hotspot mutation such as R175H restored sensitivity to erastin in HCT116 and SW48 cells (Figure S2C). These findings suggest that TP53 mutations may sensitize human CRC cells to erastin-induced ferroptosis.

We next addressed whether *TP53* deletion also affects erastin activity in CRC cells. As expected, deletion of *TP53* increased staurosporine (a classical inducer of apoptosis) resistance at 24 and 72 hr (Figure 1A) with diminished caspase-3 activity (Figure S3A) and poly (ADP-ribose) polymerase (PARP) cleavage (a major substrate of caspase-3; Figure S3B) in HCT116 cells. In contrast, loss of TP53 restored erastin sensitivity at 24 and 72 hr in HCT116 cells (Figure 1A). Live-cell imaging analysis confirmed that *TP53* deletion caused opposite effects on cell death induced by staurosporine and erastin in HCT116 cells (Movies S1, S2, S3, and S4). Moreover, depletion of TP53 by two different small hairpin RNAs (shRNAs) increased erastin-induced death at 24 and 72 hr in SW48 and HCT116 cells (Figures 1B and 1C). In contrast, TP53 depletion augmented the resistance to erastin-induced death at 24 and 72 hr in U2OS (human bone osteosarcoma) and MCF7 (human breast adenocarcinoma) cells (Figures 1B and 1C), consistent with previous reports that TP53 is a positive regulator of erastin-induced ferroptosis in non-CRC cells (Jiang et al., 2015). Transfection-enforced re-expression of WT TP53 in $TP53^{-/-}$ HCT116 cells (Figure 1D) restored staurosporine-induced death but decreased the anticancer activity of erastin (Figure 1E). Together, these observations strongly suggest that TP53 inhibits cell death induction by erastin in human CRC cells.

To determine the basis for TP53-mediated erastin resistance, we treated CRC cells with erastin in the absence or presence of inhibitors of regulated cell death. The ferroptosis inhibitors ferrostatin-1 (Dixon et al., 2012) and liproxstatin-1 (Friedmann Angeli et al., 2014) inhibited erastin-induced death of $TP53^{-/-}$ cells (Figure 1F), while ZVAD-FMK (an apoptosis inhibitor) and necrosulfonamide (a necroptosis inhibitor) failed to maintain the viability of the cells (Figure 1F). Furthermore, ferrostatin-1 and liproxstatin-1 (but not ZVAD-FMK or necrosulfonamide) abolished erastin-induced death in TP53-depleted HCT116 and SW48 cells (Figure 1F). Thus, deletion or depletion of TP53 from human CRC cells promotes erastin-induced cell death that occurs through ferroptosis.

Like erastin, SAS can induce ferroptosis by inhibition of system X_c^- activity (Dixon et al., 2012). In contrast, RSL3 (Yang

Figure 1. TP53 Inhibits Ferroptosis in Human CRC Cells

(A) $TP53^{+/+}$ and $TP53^{-/-}$ HCT116 cells were treated with staurosporine (STS; 0, 0.25, 0.5, 1, and 2 μM) or erastin (0, 5, 10, 20, and 40 μM) for 24 or 72 hr, and cell viability was assayed (n = 3, *p < 0.05, ANOVA LSD test).

(B) HCT116, SW48, MCF7, and U2OS were transfected with two different TP53 shRNAs or control shRNA for 48 hr, and the mRNA levels of TP53 after RNAi were measured with qPCR (n = 3, *p < 0.05, t test).

(C) HCT116, SW48, MCF7, and U2OS were transfected with two different TP53 shRNAs or control shRNA for 48 hr and then treated with erastin (0, 2.5, 5, 10, 20, and 40 μM) for 24 or 72 hr. The cell viability was assayed using a CCK-8 kit (n = 3, *p < 0.05, t test).

(D) Western blot analysis of TP53 expression in indicated HCT116 cells following treatment with erastin (20 μM) for 24 hours.

(E) Restored TP53 expression by gene transfection of TP53-WT cDNA in $TP53^{-/-}$ HCT116 cells increased STS-induced cell death and inhibited erastin-induced cell death (n = 3, *p < 0.05, ANOVA LSD test).

(F) Indicated CRC cells were treated with erastin in the absence or presence of ferrostatin-1, liproxstatin-1, Z-VAD-FMK, and necrosulfonamide for 24 hr, and cell viability was assayed (n = 3, *p < 0.05 versus $TP53^{+/+}$ or ctrl shRNA group, t test).

(G) Time-response analysis of cell viability from $TP53^{+/+}$ and $TP53^{-/-}$ HCT116 cells in response to erastin, SAS, RSL3, and FIN56 (n = 3, *p < 0.05 versus $TP53^{+/+}$ group, t test).

(H) Time-response analysis of cell viability and glutamate release from $TP53^{+/+}$ and $TP53^{-/-}$ HCT116 cells in response to erastin, SAS, RSL3, and FIN56 (n = 3, *p < 0.05 versus $TP53^{+/+}$ group, t test).

et al., 2014) and FIN56 (Shimada et al., 2016) can trigger ferroptosis by inhibition of glutathione peroxidase 4 (GPX4), a downstream antioxidant enzyme of System X_c^-. For comparison, we also determined the impact of *TP53* deletion in RSL3- and FIN56-induced ferroptosis in CRC cells. Unlike erastin and SAS, loss of TP53 failed to impact RSL3- and FIN56-induced growth inhibition at 24, 48, and 72 hr in HCT116 cells (Figure 1G). We confirmed the ability of erastin and SAS (but not RSL3 and FIN56) to inhibit system X_c^- by testing glutamate release into culture medium (Figure 1H). In contrast, *TP53* deletion increased the inhibition of glutamate release with or without erastin and SAS treatment (Figure 1H). These observations indicate that TP53 regulates ferroptosis via modulation of upstream signal of GPX4.

TP53 Mediates SLC7A11C Expression in Human CRC Cells

Lipid peroxidation resulting from glutathione (GSH) depletion seems to play a central role in the induction of ferroptosis (Yang and Stockwell, 2016). Therefore, we investigated whether TP53 regulates lipid peroxidation. The end products of lipid peroxidation, such as malondialdehyde (MDA), were increased following treatment with erastin in $TP53^{-/-}$ and TP53-depleted CRC cells (Figure 2A). As expected, the levels of oxidation of C11-BODIPY for the determination of lipid oxidation were increased in *TP53*-deficient cells (Figure 2B). Knockout or knockdown of TP53 also promoted erastin-induced GSH down-regulation in human CRC cells (Figure 2C). Importantly, these changes in MDA, C11-BODIPY, and GSH were reversed after transfection of *TP53* cDNA into $TP53^{-/-}$ CRC cells (Figures 2A–2C). α-Tocopherol is a lipophilic vitamin that exhibits antioxidative activity partly through increasing intracellular GSH level (Masaki et al., 2002). Treatment with α-Tocopherol or GSH limited erastin sensitivity at 24, 48, and 72 hr in $TP53^{+/+}$ and $TP53^{-/-}$ cells (Figure 2D). In contrast, induction of GSH depletion by buthionine sulfoximine (BSO) increased erastin sensitivity in $TP53^{+/+}$ and $TP53^{-/-}$ cells (Figure 2D). These findings support a role for TP53 in the control of ferroptosis-associated lipid peroxidation and antioxidative response.

System X_c^- maintains redox homeostasis by importing cystine, which is reduced to cysteine and subsequently used for the synthesis of the major antioxidant and ferroptosis inhibitor GSH (Yang et al., 2014). TP53 acts as a positive regulator of ferroptosis by transcriptionally repressing the expression of SLC7A11 (the cystine-glutamate antiporter involved in system X_c^-) in U2OS and MCF7 cells (Jiang et al., 2015). We confirmed that genetic or pharmacological inhibition of TP53 by shRNA or pifithrin-α, respectively, increased SLC7A11 mRNA (Figures 2E and 2F) and protein expression (Figures 2G and 2H) and subsequently enhanced erastin resistance (Figure 1C and 2I) in U2OS and MCF7 cells. In contrast, in human CRC cells, deletion, depletion, or pharmacological inhibition of TP53 reduced erastin-induced SLC7A11 mRNA (Figures 2E, 2F, and 2J) and protein expression (Figures 2H, 2K, and 2L) in association with increased erastin-induced cell death (Figures 1A, 1C, and 2I). Thus, TP53 has differential effects on SLC7A11 expression in CRC and non-CRC cells. In CRC cells, TP53 stimulated SLC7A11 expression, and knockdown of SLC7A11 by shRNA sensitized TP53-expressing HCT116 cells to erastin (Figure 2M and 2N).

DPP4 Mediates Ferroptosis in TP53-Deficient CRC Cells

Given that proteases play a key role in mediating cell death (Turk and Stoka, 2007), we next determined whether TP53 depletion increases ferroptosis in CRC cells by facilitating the activation of lethal proteases. Remarkably, DPP4 inhibitors (vildagliptin, alogliptin, and linagliptin), but not other protease inhibitors, completely blocked erastin-induced cell death in $TP53^{-/-}$ (Figure 3A) and TP53-depleted (Figure S4) CRC cells. Compared to $TP53^{-/-}$ cells, $TP53^{+/+}$ cells were more sensitive to H_2O_2-induced death (Figure 3A). This process was inhibited by the apoptosis inhibitor ZVAD-FMK, but not DPP4 inhibitors (vildagliptin, alogliptin, and linagliptin), indicating that DPP4 is not involved in the regulation of TP53-mediated apoptosis in oxidative injury (Figure 3A). Depletion of DPP4 with two different shRNAs or by small interfering RNA (siRNA) also reversed erastin-induced death in $TP53^{-/-}$ (Figure 3B) or TP53-depleted (Figure S5) CRC cells. These findings indicate that DPP4 is required for ferroptosis in TP53-deficient CRC cells.

The nuclear factor erythroid 2-related factor 2 (NRF2) is a transcriptional factor of the antioxidant response in various types of cell death, including ferroptosis (Sun et al., 2016b). In certain cases, DPP4 inhibitors can activate the NRF2 pathway (Wang et al., 2016a). However, the NRF2 inhibitor brusatol (Ren et al., 2011) and the alkaloid trigonelline (Arlt et al., 2013) did not restore erastin sensitivity in vildagliptin-treated $TP53^{-/-}$ HCT116 cells (Figure 3C), indicating that NRF2 is not essential for the anti-ferroptosis activity of DDP4 inhibitors.

We next asked whether TP53 regulates the expression or enzymatic activity of DPP4. Real-time qPCR (Figures 3B and S5) and immunoblot analysis (Figure 3D) revealed no significant changes in DPP4 mRNA and protein levels upon deletion or depletion of *TP53* from CRC cells. In sharp contrast, DPP4 activity increased following erastin treatment in $TP53^{-/-}$ (Figure 3E) or TP53-depleted (Figure S6) CRC cells. In contrast, vildagliptin and linagliptin inhibited DPP4 activity in $TP53^{-/-}$ CRC cells (Figure 3E). TP53 depletion failed to enhance erastin-induced DPP4 activity in U2OS and MCF7 cells (Figure S6), which expressed much lower DDP4 protein levels than HCT116 and SW48 cells (Figure S7A). Forced expression of DPP4 by gene transfection increased erastin sensitivity, especially in TP53-depleted U2OS cells (Figures S7B and S7C), indicating that the status of TP53 and DPP4 expression determines the anticancer activity of erastin.

Given that the activity of DPP4 varies in distinct subcellular compartments (Liu et al., 2014), we hypothesized that p53 might regulate the intracellular localization of DPP4. Most DPP4 is located at the plasma membrane, where it functions as a serine protease. In the nucleus, DPP4 can act as a transcription cofactor (Yamada et al., 2013). Immunoblots and enzymatic activity performed on nuclear fractions revealed an erastin-induced increase in nuclear DPP4 without enzymatic activity in $TP53^{+/+}$ (but not $TP53^{-/-}$) HCT116 cells (Figure 3F). Similarly, fluorescence microscopy confirmed that erastin-induced nuclear accumulation depended on TP53 (Figures S8A and S8B). Collectively, these findings suggest that TP53 favors the subcellular

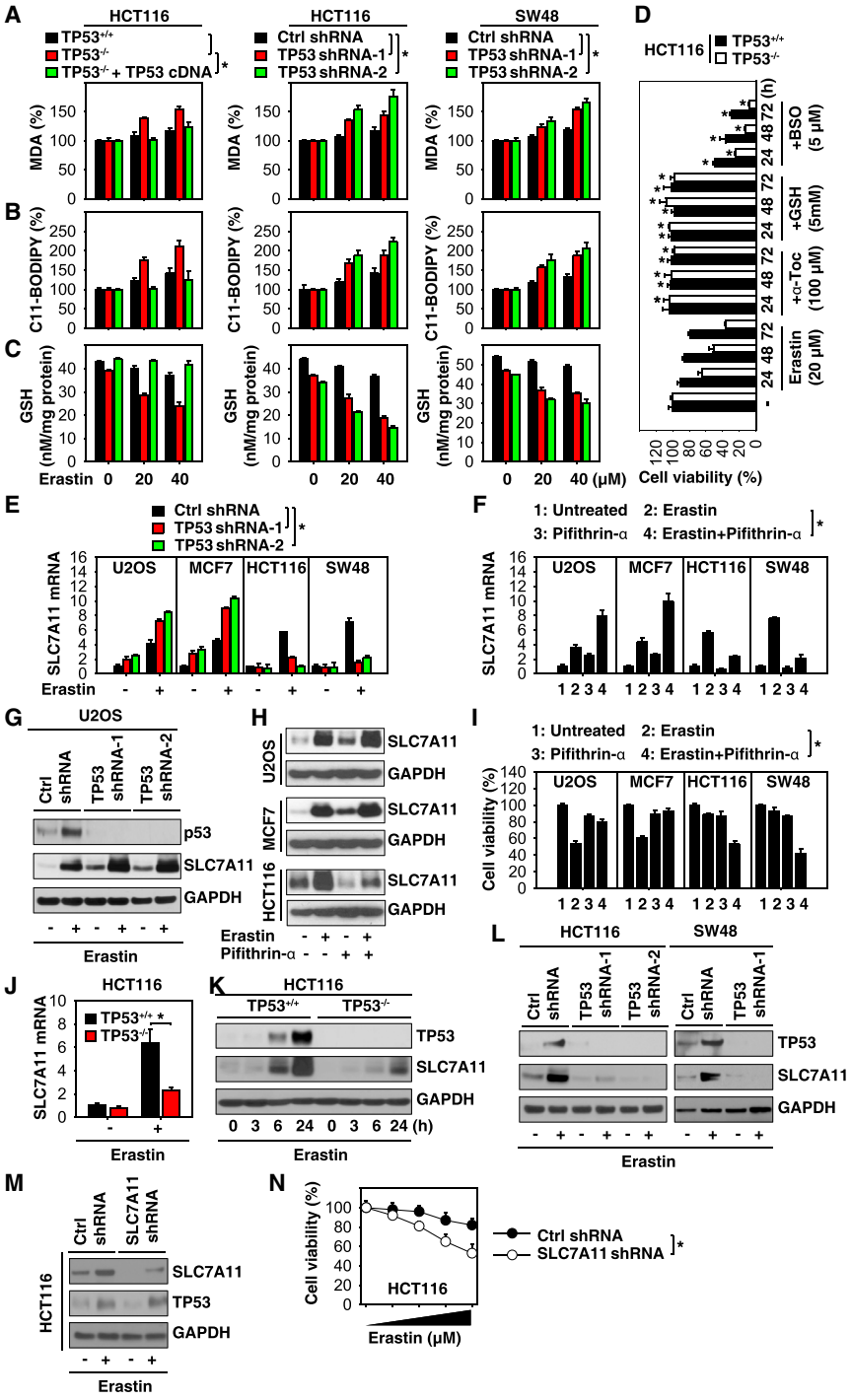

Figure 2. TP53 Mediates SLC7A11C Expression in Human CRC Cells

(A–C) Indicated CRC cells were treated with erastin (20 and 40 μM) for 24 hr. The levels of MDA (A), oxidized C11-BODIPY (B), and GSH (C) were assayed (n = 3, *p < 0.05, t test).

(D) Effects of α-tocopherol (α-Toc), GSH, and BSO on erastin sensitivity in *TP53*$^{+/+}$ and *TP53*$^{-/-}$ cells (n = 3, *p < 0.05, t test).

(E) qPCR analysis of SLC7A11 mRNA in indicated cells following treatment with erastin (20 μM) for 24 hr (n = 3, *p < 0.05, t test).

(F) qPCR analysis of SLC7A11 mRNA in indicated cells following treatment with erastin (20 μM) in the absence or presence of pifithrin-α (5 μM) for 24 hr (n = 3, *p < 0.05, t test).

(G) Western blot analysis of SLC7A11 expression in TP53-WT and TP53-knockdown U2OS cells following treatment with erastin (20 μM) for 24 hr.

(H) Indicated cells were treated with erastin (20 μM) in the absence or presence of pifithrin-α (5 μM) for 24 hr. SLC7A11 protein levels were assayed using western blot.

(I) Indicated cells were treated with erastin (20 μM) in the absence or presence of pifithrin-α (5 μM) for 24 hr, and then cell viability was assayed (n = 3, *p < 0.05, t test).

(J) qPCR analysis of SLC7A11 mRNA in indicated cells following treatment with erastin (20 μM) for 24 hr (n = 3, *p < 0.05, t test).

(K) Knockout of p53 inhibited erastin (20 μM, 24 hr)-induced SLC7A11 protein expression in human CRC cells.

(L) Knockdown of p53 inhibited erastin (20 μM, 24 hr)-induced SLC7A11 protein expression in human CRC cells.

(M) Western blot analysis of SLC7A11 expression in indicated HCT116 cells following treatment with erastin (20 μM) for 24 hours.

(N) Knockdown of SLC7A11 by shRNA sensitized TP53-expressing HCT116 cells to erastin (0–40 μM, 24 hr, n = 3, *p < 0.05, ANOVA LSD test).

redistribution of DPP4 toward a nuclear, enzymatically inactive pool.

The NADPH oxidase (NOX) protein family transfers electrons across biological membranes to reduce oxygen to superoxide. Increased NADPH-mediated ROS production by NOX1 contributes to erastin-induced ferroptosis (Dixon et al., 2012). We observed that NOX activity and MDA production were remarkably upregulated in *TP53*$^{-/-}$ (Figure 3G) and TP53-depleted (Figures S8C and S8D) cells following erastin treatment. In contrast, treatment with DPP4 inhibitors (vildagliptin or linagliptin) or shRNA-mediated depletion of DPP4 diminished erastin-induced NOX activity and MDA production in *TP53*$^{-/-}$ (Figure 3G) and TP53-depleted CRC cells (Figures S8C and S8D). Interestingly, genetic depletion of DPP4 (but not pharmacologic inhibition of DPP4) by shRNA upregulated SLC7A11 mRNA expression in *TP53*$^{+/+}$, but not *TP53*$^{-/-}$, HCT116 cells (Figure 3G), suggesting that the expression and activity of DPP4 may play different roles in the regulation of SLC7A11 mRNA expression in *TP53*$^{+/+}$ CRC cells. Moreover, NOX1 and DPP4 co-immunoprecipitated in *TP53*$^{-/-}$ (but not *TP53*$^{+/+}$) HCT116 cells following treatment with erastin (Figure 3H). This interaction was blocked in the

A

Target	Compound	Target	Compound
DPP4	Vildagliptin	HCV	VX-222
DPP4	Linagliptin	γ-secretase	Semagacestat
DPP4	Alogliptin	Cysteine	Z-FA-FMK
MMP	Doxycycline	Cathepsin K	Odanacatib
HIV	Ritonavir	Caspase	ZVAD-FMK
HIV	Atazanavir	β-amyloid	DAPT

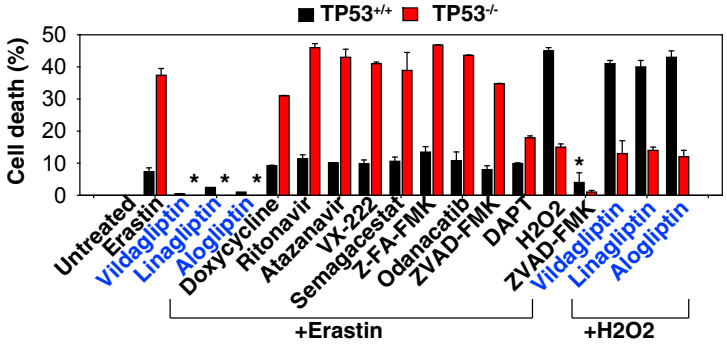

B

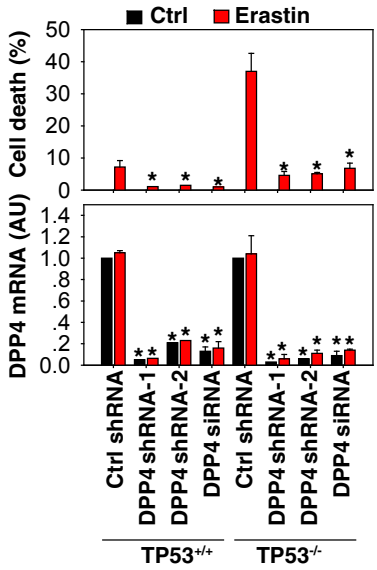

C

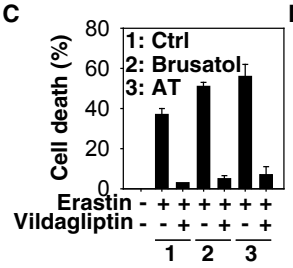

D

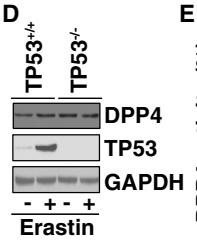

E

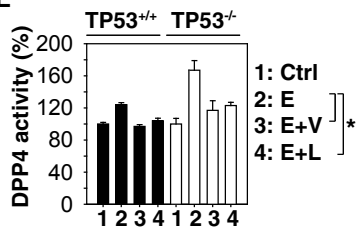

F

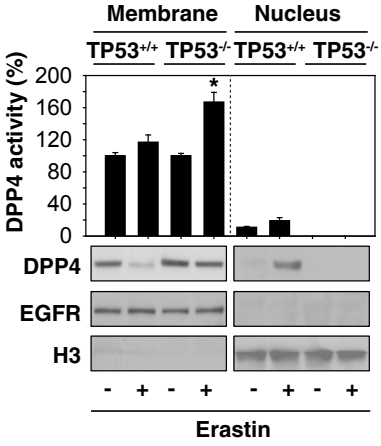

G

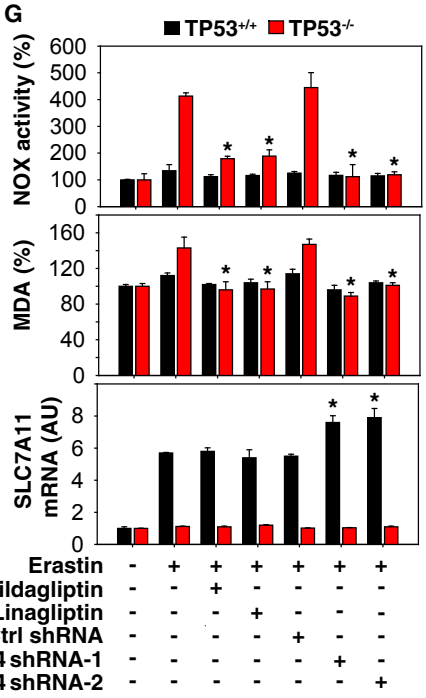

H

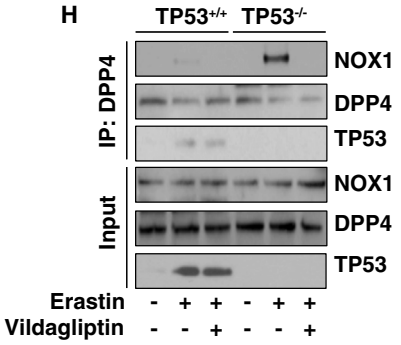

I

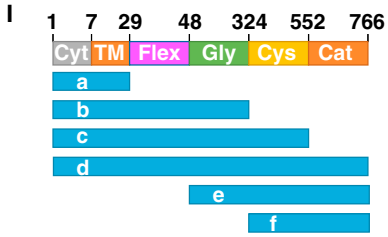

J

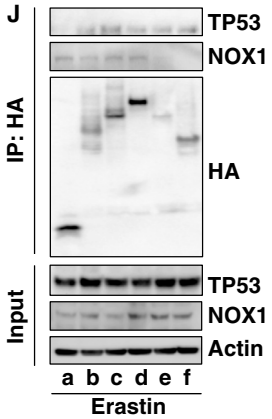

K

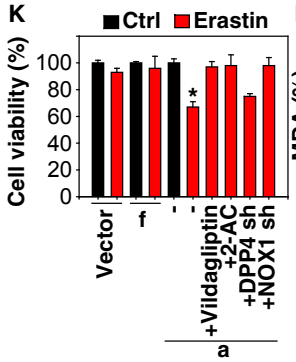

L

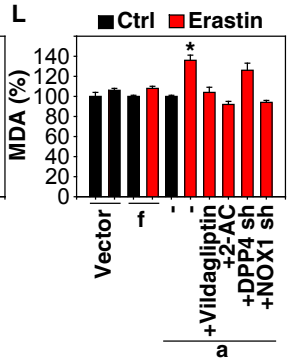

(legend on next page)

presence of the DPP4 inhibitor vildagliptin (Figure 3H). In contrast, vildagliptin had no effect on the erastin-induced interaction between DPP4 and TP53 in WT HCT116 (Figure 3H). Together, these findings indicate that the interaction between DPP4 and NOX1 is required for lipid peroxidation in ferroptosis in TP53-deficient (but not TP53-sufficient) CRC cells.

Human DPP4 has 766 amino acids, including an extracellular portion (29–766 aa), a transmembrane region (TM; 7–29 aa), and an intracellular tail (Cyt; 1–7 aa) (Figure 3I). The extracellular portion of DPP4 contains a flexible segment (Flex; 29–48 aa), a glycosylation domain (Gly; 48–324 aa), a cysteine-rich domain (Cys; 324–552 aa), and a catalytic domain (Cat; 552–766 aa). We performed an in-depth analysis of the structural basis of DPP4 responsible for the interaction between DPP4 and TP53. We constructed a series of vectors that express full-length or various fragment mutants of DPP4 (1–29 aa, 1–324 aa, 1–552 aa, 1–766 aa, 48–766 aa, and 324–766 aa) based on its structure. Immunoprecipitation assays showed that 1–29 aa was the sole fragment that failed to bind to TP53 upon transfection into cells (Figure 3J). In contrast, 1–48 aa was required for binding to NOX1 (Figure 3J). Transfection-enforced expression of 1–29 aa rendered TP53-expressing HCT116 cells susceptible to erastin-induced cell death (Figure 3K) with increased lipid peroxidation (Figure 3L). This process was inhibited by the DPP4 inhibitor vildagliptin, the NOX1 inhibitor 2-acetylphenothiazine (2-AC), or shRNA-mediated depletion of NOX1 (Figures 3K and 3L). In contrast, knockdown of DPP4 by shRNA had no effect on 1- to 29-aa-mediated erastin sensitivity and lipid peroxidation in TP53-expressing HCT116 cells (Figures 3K and 3L). Collectively, these findings further support that the formation of DPP4-TP53 complex limits ferroptosis, whereas the DPP4-NOX1 complex promotes ferroptosis. Moreover, the 1- to 29-aa fragment of DPP4 does not require endogenous DPP4 to become sensitized to ferroptosis.

Loss of TP53 Enhances the Anticancer Activity of Erastin *In Vivo*

We investigated whether loss of TP53 enhances the anticancer activity of erastin *in vivo*. *TP53*$^{-/-}$ HCT116 CRC cells were implanted subcutaneously into the right flank of immunodeficient mice. One week later, tumor-bearing mice were treated with erastin with or without the DPP4 inhibitor vildagliptin. Erastin effectively reduced the growth of tumors formed (Figures 4A–4C) by *TP53*$^{-/-}$ (but not *TP53*$^{+/+}$) HCT116 cells as it locally increased MDA levels (Figure 4D), as well as the enzymatic activities of DPP4 (Figure 4E) and NOX (Figure 4F). Erastin treatment of *TP53*$^{-/-}$ (but not *TP53*$^{+/+}$) CRC also suppressed the expression of SLC7A11 mRNA (Figure 4G) and upregulated cation transport regulator-like protein 1 (CHAC1), a biomarker associated with ferroptosis (Dixon et al., 2014) (Figure 4H). Importantly, the DPP4 inhibitor vildagliptin attenuated the anticancer activity of erastin on *TP53*$^{-/-}$ CRC and reversed all effects of erastin on intratumoral MDA levels (Figure 4D), DPP4 activity (Figure 4E), NOX activity (Figure 4F), SLC7A11 mRNA (Figure 4G), and CHAC1 mRNA (Figure 4H). These observations suggest that TP53 inactivation sensitizes human CRC cells to erastin-induced ferroptosis by exacerbated activation of the DPP4 pathway and subsequent lipid peroxidation *in vivo*.

We next determined whether *TP53* mutation status determines the anticancer activity of erastin in CRC cells *in vivo*. Consistent with our *in vitro* observations, we found that human CRC cell lines with a *TP53* mutation (CACO2, DLD1, and SW387) were more sensitive to erastin-mediated tumor suppression than *TP53* WT cell lines (HCT116 and SW48) (Figure 4I). This process was associated with increased intratumoral MDA levels (Figure 4J), DPP4 activity (Figure 4K), and NOX activity (Figure 4L) and decreased SLC7A11 mRNA (Figure 4M) and upregulated CHAC1 mRNA (Figure 4N) in *TP53*-mutated CRC cell lines. These findings support that TP53 mutation contributes to ferroptosis *in vivo*.

To further determine the relationships among DPP4, SLC7A11, and TP53 in the regulation of ferroptosis *in vivo*, we stably knocked down *DPP4* or *SLC7A11* in *TP53*$^{+/+}$ or *TP53*$^{-/-}$ HCT116 cells (Figure 5A). *TP53*$^{+/+}$*DPP4*^{KD}, *TP53*$^{-/-}$*DPP4*^{KD}, and *TP53*$^{+/+}$ HCT116 cells were more resistant to erastin-mediated tumor suppression than *TP53*$^{-/-}$, *TP53*$^{+/+}$*SLC7A11*^{KD}, and *TP53*$^{-/-}$*SLC7A11*^{KD} HCT116 cells (Figure 5B). The mRNA levels of CHAC1 were elevated in *TP53*$^{-/-}$, *TP53*$^{+/+}$*SLC7A11*^{KD}, and *TP53*$^{-/-}$*SLC7A11*^{KD} HCT116 cells following erastin treatment (Figure 5C), indicating that increased ferroptosis occurs in these tumors.

Figure 3. DPP4 Mediates Ferroptosis in TP53-Deficient CRC Cells

(A) A DPP4 inhibitor, but not the other protease inhibitors indicated, at 10 μM blocked erastin (20 μM, 24 hr)-induced cell death in *TP53*$^{-/-}$ HCT116 cells (n = 3, *p < 0.05 versus the erastin group, t test). Cell death was analyzed by propidium iodide staining.

(B) Knockdown of DPP4 by shRNAs inhibited erastin-induced cell death in *TP53*$^{-/-}$ HCT116 cells (n = 3, *p < 0.05 versus the control shRNA group, t test).

(C) The NRF2 inhibitor brusatol (100 nM) and the alkaloid trigonelline (AT; 0.5 μM) did not restore erastin (20 μM, 24 hr) sensitivity in vildagliptin-treated *TP53*$^{-/-}$ HCT116 cells.

(D) Western blot analysis of DDP4 expression in *TP53*$^{+/+}$ and *TP53*$^{-/-}$ HCT116 cells with or without 24-hr erastin (20 μM) treatment.

(E) Loss of TP53 increased erastin (20 μM)-induced DDP4 activation at 24 hr (n = 3, *p < 0.05 versus TP53+/+ group, t test). E, erastin; V, vidagliptin; L, linagliptin.

(F) Loss of TP53 increased erastin (20 μM)-induced nuclear DPP4 accumulation at 24 hr (n = 3, *p < 0.05 versus TP53+/+ group, t test).

(G) Pharmacologic and genetic inhibition of DPP4 limited erastin (20 μM)-induced NOX activation and MDA production at 24 hr in *TP53*$^{-/-}$ HCT116 cells (n = 3, *p < 0.05 versus the *TP53*$^{+/+}$ group, t test).

(H) Immunoprecipitation (IP) analysis of DPP4 protein complex in *TP53*$^{+/+}$ and *TP53*$^{-/-}$ HCT116 cells with or without 24-hr erastin (20 μM) and vidagliptin (10 μM) treatment.

(I) Schematic showing the domain structure and mutants of DPP4.

(J) IP analysis of the DPP4-TP53 complex in HCT116 cells transfected with hemagglutinin (HA)-tagged DPP4 WT or fragments with 24-hr erastin (20 μM) treatment.

(K and L) 1–29 aa of DPP4 renders TP53-expressing HCT116 cells susceptible to erastin (20 μM, 24 hr)-induced cell death (K) and lipid peroxidation (L) (n = 3, *p < 0.05 versus the control group, t test).

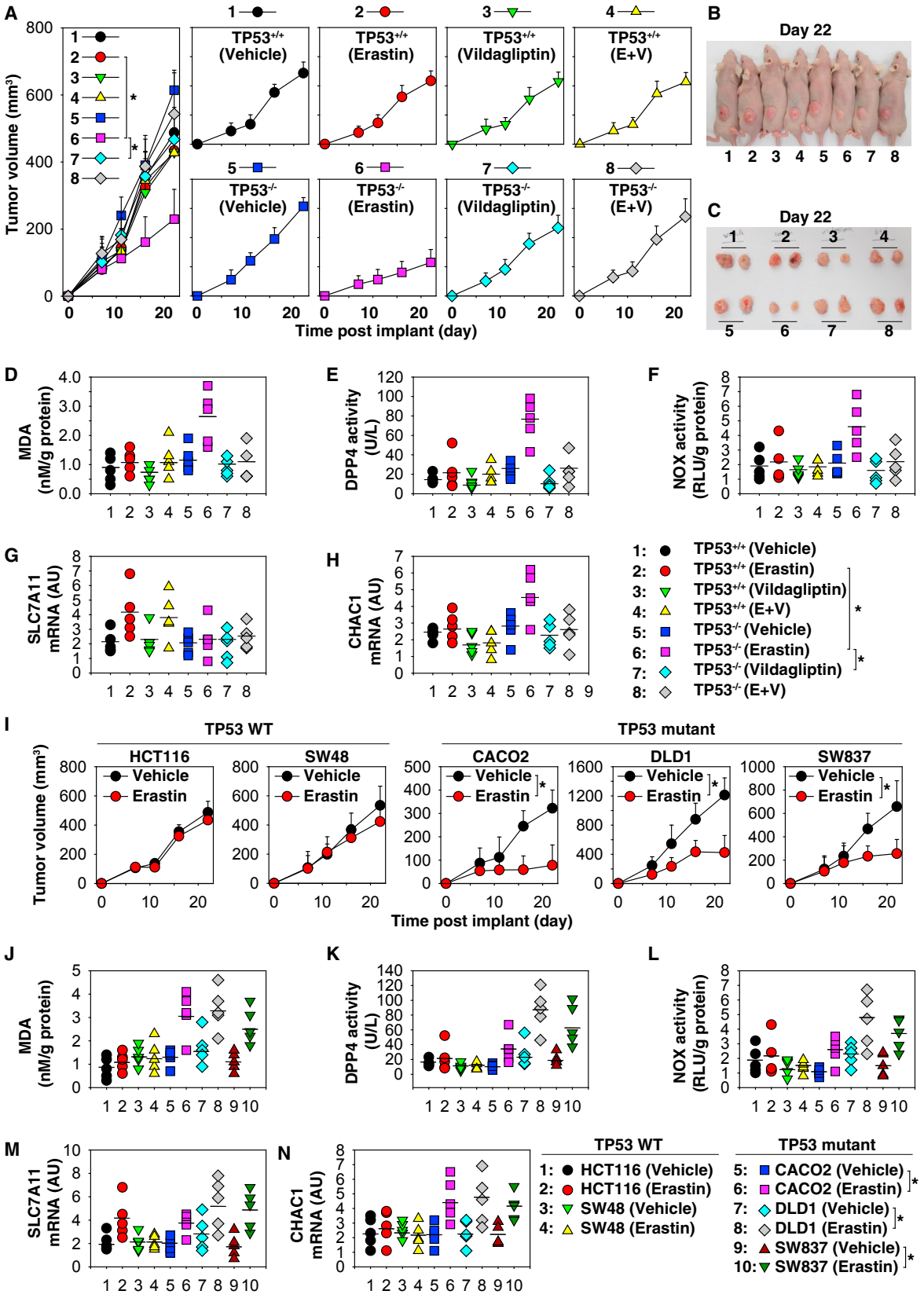

(legend on next page)

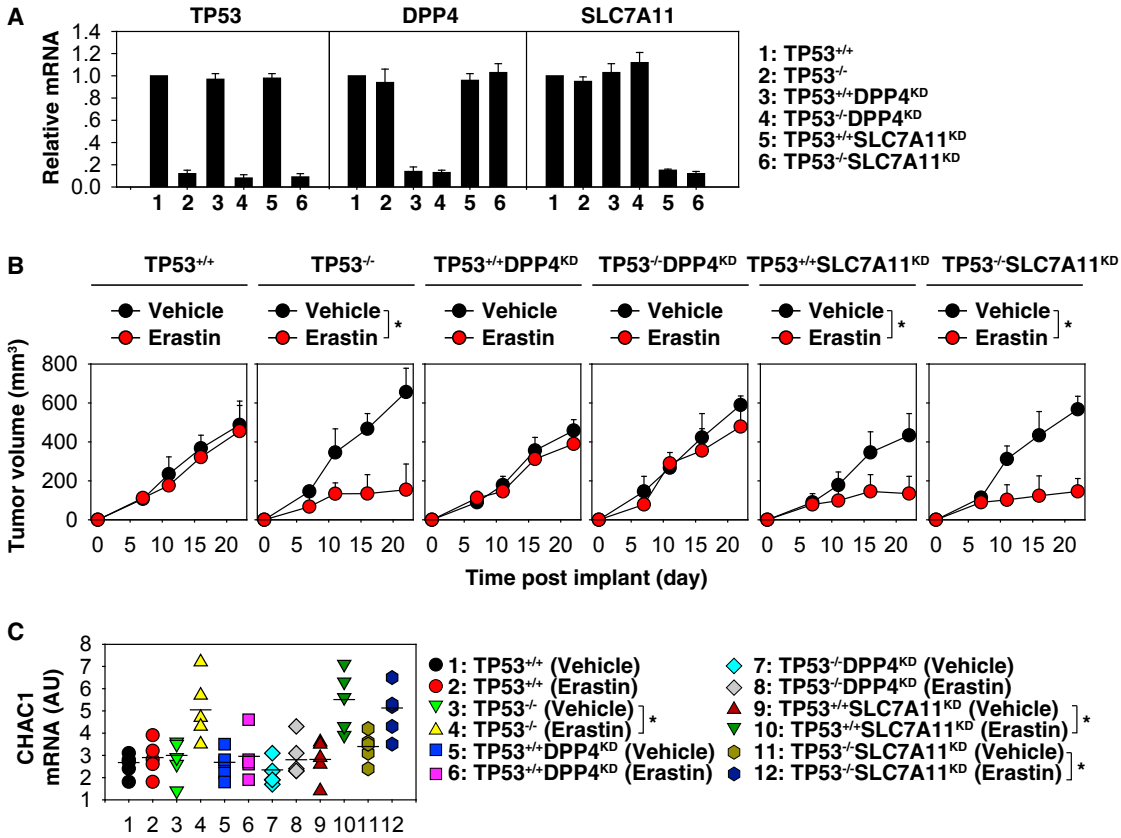

Figure 5. Role of TP53, DPP4, and SLC7A11 in the Regulation of Anticancer Activity of Erastin *In Vivo*

(A) qPCR analysis of TP53, DPP4, and SLC7A11 expression in HCT116 cells.

(B) Athymic nude mice were injected subcutaneously with HCT116 cells and treated with erastin (40 mg/kg intraperitoneal injection, twice every other day) at day 7 for 2 weeks. Tumor volume was calculated weekly (n = 5 mice/group, data expressed as means ± SD, *p < 0.05, ANOVA LSD test).

(C) In parallel, CHAC1 mRNA levels in the isolated tumors at day 22 were assayed (n = 5 mice/group, *p < 0.05, t test).

DISCUSSION

The concept of precision medicine has recently been exploited in various efforts to develop new genotype-selective anticancer agents (Friedman et al., 2015). Members of the small GTPase RAS family (K-RAS, H-RAS, and N-RAS) are mutated in one-third of all human cancers, thus representing an important target for anti-cancer drug development (Cox et al., 2014). Ferroptosis was originally identified as a form of non-apoptotic regulated cell death that selectively eliminates cancer cells with RAS mutations via a cell-permeable compound termed erastin, leading to the proposal that erastin might be used to treat RAS-mutated cancers (Dixon et al., 2012; Dolma et al., 2003). Here, we demonstrate that TP53 (but not R-RAS) is a key regulator of erastin-induced ferroptosis in CRC cells.

Consistent with our findings that R-RAS is dispensable for erastin-induced ferroptosis in CRC cells, several normal RAS WT cells such as kidney tubule cells, T cells, and fibroblasts

Figure 4. Loss of TP53 Enhances the Anticancer Activity of Erastin *In Vivo*

(A) *TP53*$^{-/-}$ HCT116 cells were more sensitive to erastin *in vivo*. Athymic nude mice were injected subcutaneously with *TP53*$^{+/+}$ and *TP53*$^{-/-}$ HCT116 cells (4×10^6 cells/mouse) and treated with erastin (40 mg/kg intraperitoneal injection, twice every other day), vildagliptin (20 mg/kg oral administration, once every other day), or combination treatment (erastin plus vildagliptin) at day 7 for 2 weeks. Tumor volume was calculated weekly (n = 10 mice/group, data expressed as means ± SD, *p < 0.05, ANOVA LSD test).

(B and C) Representative photographs of tumor-bearing mice (B) and isolated tumors (C) at day 22.

(D–H) In parallel, MDA levels (D), DPP4 activity (E), NOX activity (F), SLC7A11 mRNA (G), and CHAC1 mRNA (H) in the isolated tumors were assayed (n = 5 mice/group, *p < 0.05, t test).

(I) Athymic nude mice were injected subcutaneously with indicated human CRC cells (4×10^6 cells/mouse) and treated with erastin (40 mg/kg intraperitoneal injection, twice every other day) at day 7 for 2 weeks. Tumor volume was calculated weekly (n = 10 mice/group, data expressed as means ± SD, *p < 0.05, ANOVA LSD test).

(J–N) In parallel, MDA levels (J), DPP4 activity (K), NOX activity (L), SLC7A11 mRNA (M), and CHAC1 mRNA (N) in the isolated tumors at day 22 were assayed (n = 5 mice/group, *p < 0.05, t test).

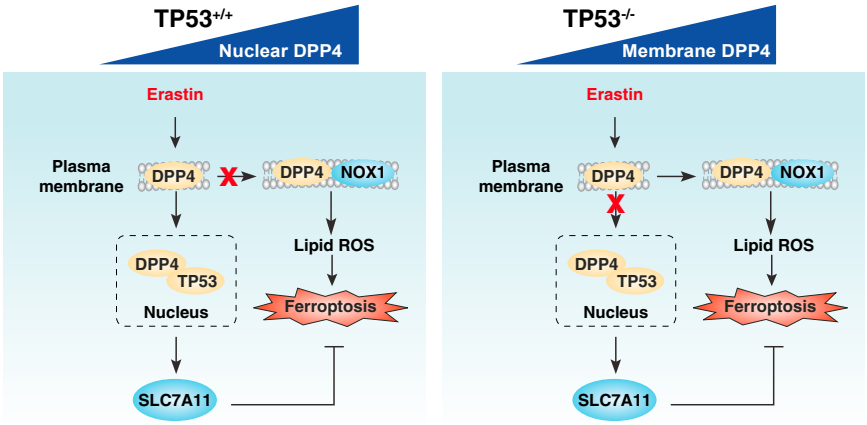

Figure 6. Schematic Depicting the Interplay between TP53 and DDP4 in the Regulation of Erastin-Induced Ferroptosis in Human CRC Cells

Loss of TP53 prevents nuclear accumulation of DPP4 and then triggers membrane-associated DPP4-mediated lipid peroxidation, which finally results in ferroptosis.

are sensitive to erastin (Friedmann Angeli et al., 2014; Jiang et al., 2015; Linkermann et al., 2014; Matsushita et al., 2015; Skouta et al., 2014). Even in some cases, overexpression of mutant RAS in rhabdomyosarcoma cells (e.g., RMS13 cells) promotes ferroptosis resistance to erastin and RLS3 (Schott et al., 2015). Thus, RAS-independent and RAS-dependent pathways in ferroptosis may differ significantly by tumor type.

In contrast, our study demonstrates that TP53 is a negative regulator of ferroptosis in human CRC cells. Although TP53-WT CRC cells are sensitive to apoptotic stimuli, normal TP53-WT CRC cells are resistant to erastin-induced ferroptosis because of the induction of TP53 expression. In contrast, genetic or pharmacologic inhibition of TP53 or knockin of TP53 hotspot mutant (e.g., R175H) restores sensitivity to erastin-induced ferroptosis. As expected, these TP53-deficient CRC cells are resistant to apoptosis. Given that intrinsic or acquired resistance to apoptosis is one of the hallmarks of CRC (Huerta et al., 2006), our *in vitro* and *in vivo* findings highlight the urgent need to develop approaches to trigger ferroptosis as a strategy to eliminate TP53-deficent CRC cells.

TP53-mediated metabolic changes that occur in cancer cells have been studied for several decades, but our appreciation of the complexity and importance of those changes is only now being realized (Humpton and Vousden, 2016; Parrales and Iwakuma, 2016; Puzio-Kuter, 2011; Vousden and Ryan, 2009). Our current study and other reports demonstrate a capacity for TP53 to fine-tune lipid peroxidation in ferroptosis (Jennis et al., 2016; Jiang et al., 2015; Ou et al., 2016). Activation of p53 has been found to be required for ferroptosis in certain non-CRC cancer cells (Jiang et al., 2015). This process depends on transcriptional inhibition of SLC7A11, a key component of antioxidant system X_c^- (Jiang et al., 2015), or transcriptional induction of spermidine/spermine N^1-acetyltransferase 1 and glutaminase 2, two genes involved in lipid peroxidation (Jennis et al., 2016; Ou et al., 2016). Our study indicates that TP53-mediated SLC7A11 expression contributes to ferroptosis resistance in TP53-WT CRC cells. This process is regulated by the DPP4-TP53 complex; disrupting this complex can restore ferroptosis sensitivity in CRC cells. The E3 ubiquitin ligase murine double minute-2 (MDM2) regulates the proteasomal degradation of p53. However, inhibition of ferroptosis by ferrostatin-1 cannot prevent MDM2-depletion-induced cell death in podocytes (Thomasova et al., 2015), suggesting the additional possibility that MDM2 may play a different role in ferroptosis.

A key finding in our study is the contribution of DPP4 (also termed CD26) to ferroptosis. We demonstrated that loss of TP53 prevents nuclear accumulation of DPP4 in CRC cells and thus facilitates plasma-membrane-associated DPP4-dependent lipid peroxidation, which finally results in ferroptosis. Beyond diabetes, the role of DPP4 has been widely studied in several types of cancer, including CRC. The expression of DPP4 correlated with the populations of cancer stem cells and poor survival in human CRC (Lam et al., 2014; Pang et al., 2010). DPP4 has peptidase activity and is able to cleave and degrade many biologically active peptides (Tanaka et al., 1992). We demonstrate that the enzyme activity of DPP4 is not essential for ferroptosis induction. DPP4 also has other non-enzymatic functions, interacting with different partners and sustaining tumor growth, invasion, and metastasis (Havre et al., 2008). Consistent with this idea, we found that DPP4-NOX binding is required for lipid peroxidation in ferroptosis. DPP4 inhibitors can target both enzymatic and non-enzymatic functions of DPP4 (Chen et al., 2015; Deacon and Lebovitz, 2016; Fadini and Avogaro, 2011; Jackson, 2017; Zhong et al., 2013). The context-dependent effects of DPP4 inhibitors need to be explored further.

In summary, the results of our study establish that TP53 antagonizes ferroptosis in CRC cells by favoring the localization of DPP4 toward a nuclear, enzymatically inactive pool (Figure 6). This pathway is different from the previously identified function of TP53 as a positive regulator of ferroptosis in non-CRC cells (Jennis et al., 2016; Jiang et al., 2015; Ou et al., 2016; Wang et al., 2016b). Therefore, the bidirectional control of ferroptosis by p53 through transcription-dependent and transcription-independent mechanisms is tumor-type dependent. Our current data also support an emerging anticancer strategy and suggest that pharmacological induction of ferroptosis may be effective in genotype-selected subgroups of CRC patients. In particular, the presence of two genotypes associated with poor prognosis in CRC—namely, TP53 mutation/deletion (Fearon, 2011) combined with DPP4 overexpression (Lam et al., 2014) —is likely to characterize a target population that would profit from treatment with erastin and perhaps other yet-to-be-developed ferroptosis inducers. Identification and characterization of unknown nuclear localization signals in DPP4 could be important in understanding the location-dependent role of DPP4 in ferroptosis.

EXPERIMENTAL PROCEDURES

Reagents

Erastin (#S7242), ferrostatin-1 (#S7243), liproxstatin-1 (#S7699), staurosporine (#S1421), pifithrin-α (#S2929), vildagliptin (#S3033), alogliptin (#S2868), linagliptin (#S3031), doxycycline (#S4163), ritonavir (#S1185), atazanavir sulfate (#S1457), VX-222 (#S1480), semagacestat (#S1594), Z-FA-FMK (#S7391), odanacatib (#S1115), and DAPT (#S2215) were purchased form Selleck Chemicals (Houston, TX, USA). Z-VAD-FMK (#219007) was purchased from EMD Millipore Corporation (Darmstadt, Germany). Necrosulfonamide (#5025) was purchased from Tocris Bioscience (Avonmouth, Bristol, UK). 2-acetylphenothiazine (#175226), alkaloid trigonelline (#T5509), brusatol (#SML1868), α-tocopherol (#258024), BSO (#19176), and GSH (#1294820) were purchased from Sigma-Aldrich (St. Louis, MO, USA).

Cell Culture

Human CRC cell lines (HCT116, SW48, CACO2, DLD1, and SW837), the human osteosarcoma cell line U2OS, and the human breast cancer cell line MCF7 were purchased from the American Type Culture Collection (Manassas, VA, USA). K-RAS$^{+/G13D}$, K-RAS$^{-/G13D}$, and K-RAS$^{+/-}$ HCT116 cells, and K-RAS$^{+/+}$ and K-RAS$^{G12D/+}$ SW48 cells were purchased from Horizon Discovery (Waterbeach, Cambridge, UK). TP53$^{+/+}$ and TP53$^{-/-}$ HCT116 cells were a kind gift from Dr. Bert Vogelstein (Johns Hopkins Kimmel Cancer Center, Baltimore, MD, USA). These cells were cultured in McCoy's 5a Medium (CRC cell lines and U2OS) or Eagle's minimum essential medium (MCF7) supplemented with 10% heat-inactivated fetal bovine serum and 100 U penicillin and 100 μg/mL streptomycin at 37°C, 95% humidity, and 5% CO_2. The cell culture mediums and supplements were purchased from Thermo Fisher Scientific (Grand Island, NY, USA). All cells were mycoplasma-free and authenticated using short tandem repeat DNA profiling analysis.

Animal Model

All animal experiments were approved by the University of Pittsburgh and the Third Affiliated Hospital of Guangzhou Medical University Institutional Animal Care and Use Committees and performed in accordance with the Association for Assessment and Accreditation of Laboratory Animal Care guidelines (https://www.aaalac.org). All mice were housed on a 12-hr light/dark cycle at a controlled temperature (21°C –23°C) and provided with a standard rodent diet and water ad libitum throughout all experiments.

To generate subcutaneous tumors, 4 × 10^6 CRC cell lines in 100 μL PBS were injected subcutaneously to the right of the dorsal midline in male or female athymic nude mice (8–10 weeks old and weighing 22–25 g). Once the tumors reached 50–70 mm^3 at day 7, mice were randomly allocated into groups and treated with erastin (40 mg/kg/ intraperitoneal injection, twice every other day), vildagliptin (20 mg/kg oral administration, once every other day), or combination treatment (erastin plus vildagliptin) for 2 weeks. On day 22 after the start of treatment, tumors were removed. Tumors were measured twice weekly, and volumes were calculated using the formula length × $width^2$ × π/6.

Statistical Analysis

Data are expressed as means ± SD of three independent experiments. The significance of differences between groups was determined using ANOVA least significant difference (LSD) or t tests. A p value < 0.05 was considered statistically significant.

Full methods are available in Supplemental Experimental Procedures.

SUPPLEMENTAL INFORMATION

Supplemental Information includes Supplemental Experimental Procedures, eight figures, and four movies and can be found with this article online at http://dx.doi.org/10.1016/j.celrep.2017.07.055.

AUTHOR CONTRIBUTIONS

Experiments were conceived and designed by D.T. and G.K. Experiments were performed by Y.X., S.Z., X.S., Y.F., H.Y., J.L., X.S., R.K., and D.T. Data were analyzed by Y.X., M.Z., L.Z., T.R.B., M.T.L., H.J.Z., R.K., G.K., and D.T. The paper was written by Y.X., G.K., and D.T. L.Z., T.R.B., M.T.L., and H.J.Z. edited and commented on the manuscript.

ACKNOWLEDGMENTS

We thank Christine Heiner (Department of Surgery, University of Pittsburgh) for her critical reading of the manuscript. This work was supported by grants from the US NIH (R01GM115366, R01CA160417, and R01CA181450), the Natural Science Foundation of Guangdong Province (2016A030308011), the American Cancer Society (research scholar grant RSG-16-014-01-CDD), the National Natural Science Foundation of China (31671435, 81400132, and 8177100253), the National Funds of Developing Local Colleges and Universities Grant (B16056001), a Frontier and Key Technology Innovation Special Grant from the Department of Science and Technology of Guangdong Province (2016B030229008), and the Guangdong Province Universities and Colleges Pearl River Scholar Funded Scheme (2017). This project partly utilized University of Pittsburgh Cancer Institute shared resources supported by award P30CA047904. G.K. is supported by the Ligue contre le Cancer (équipe labelisée); Agence National de la Recherche (ANR) Projets blancs; ANR under the frame of E-Rare-2, the ERA-Net for Research on Rare Diseases; Association pour la recherche sur le cancer (ARC); Cancéropôle Ile-de-France; Institut National du Cancer (INCa); Institut Universitaire de France; Fondation pour la Recherche Médicale (FRM); the European Commission (ArtForce); the European Research Council (ERC); the LeDucq Foundation; the LabEx Immuno-Oncology; the RHU Torino Lumière; the SIRIC Stratified Oncology Cell DNA Repair and Tumor Immune Elimination (SOCRATE); the SIRIC Cancer Research and Personalized Medicine (CARPEM); and the Paris Alliance of Cancer Research Institutes (PACRI).

Received: April 26, 2017
Revised: June 29, 2017
Accepted: July 19, 2017
Published: August 15, 2017

REFERENCES

Arlt, A., Sebens, S., Krebs, S., Geismann, C., Grossmann, M., Kruse, M.L., Schreiber, S., and Schäfer, H. (2013). Inhibition of the Nrf2 transcription factor by the alkaloid trigonelline renders pancreatic cancer cells more susceptible to apoptosis through decreased proteasomal gene expression and proteasome activity. Oncogene *32*, 4825–4835.

Bieging, K.T., Mello, S.S., and Attardi, L.D. (2014). Unravelling mechanisms of p53-mediated tumour suppression. Nat. Rev. Cancer *14*, 359–370.

Chen, X.W., He, Z.X., Zhou, Z.W., Yang, T., Zhang, X., Yang, Y.X., Duan, W., and Zhou, S.F. (2015). Clinical pharmacology of dipeptidyl peptidase 4 inhibitors indicated for the treatment of type 2 diabetes mellitus. Clin. Exp. Pharmacol. Physiol. *42*, 999–1024.

Cox, A.D., Fesik, S.W., Kimmelman, A.C., Luo, J., and Der, C.J. (2014). Drugging the undruggable RAS: Mission possible? Nat. Rev. Drug Discov. *13*, 828–851.

Deacon, C.F., and Lebovitz, H.E. (2016). Comparative review of dipeptidyl peptidase-4 inhibitors and sulphonylureas. Diabetes Obes. Metab. *18*, 333–347.

Dixon, S.J., Lemberg, K.M., Lamprecht, M.R., Skouta, R., Zaitsev, E.M., Gleason, C.E., Patel, D.N., Bauer, A.J., Cantley, A.M., Yang, W.S., et al. (2012). Ferroptosis: an iron-dependent form of nonapoptotic cell death. Cell *149*, 1060–1072.

Dixon, S.J., Patel, D.N., Welsch, M., Skouta, R., Lee, E.D., Hayano, M., Thomas, A.G., Gleason, C.E., Tatonetti, N.P., Slusher, B.S., and Stockwell, B.R. (2014). Pharmacological inhibition of cystine-glutamate exchange induces endoplasmic reticulum stress and ferroptosis. eLife *3*, e02523.

Doll, S., Proneth, B., Tyurina, Y.Y., Panzilius, E., Kobayashi, S., Ingold, I., Irmler, M., Beckers, J., Aichler, M., Walch, A., et al. (2017). ACSL4 dictates ferroptosis sensitivity by shaping cellular lipid composition. Nat. Chem. Biol. *13*, 91–98.

Dolma, S., Lessnick, S.L., Hahn, W.C., and Stockwell, B.R. (2003). Identification of genotype-selective antitumor agents using synthetic lethal chemical screening in engineered human tumor cells. Cancer Cell *3*, 285–296.

Eling, N., Reuter, L., Hazin, J., Hamacher-Brady, A., and Brady, N.R. (2015). Identification of artesunate as a specific activator of ferroptosis in pancreatic cancer cells. Oncoscience *2*, 517–532.

Fadini, G.P., and Avogaro, A. (2011). Cardiovascular effects of DPP-4 inhibition: beyond GLP-1. Vascul. Pharmacol. *55*, 10–16.

Fearon, E.R. (2011). Molecular genetics of colorectal cancer. Annu. Rev. Pathol. *6*, 479–507.

Friedman, A.A., Letai, A., Fisher, D.E., and Flaherty, K.T. (2015). Precision medicine for cancer with next-generation functional diagnostics. Nat. Rev. Cancer *15*, 747–756.

Friedmann Angeli, J.P., Schneider, M., Proneth, B., Tyurina, Y.Y., Tyurin, V.A., Hammond, V.J., Herbach, N., Aichler, M., Walch, A., Eggenhofer, E., et al. (2014). Inactivation of the ferroptosis regulator Gpx4 triggers acute renal failure in mice. Nat. Cell Biol. *16*, 1180–1191.

Green, D.R., and Kroemer, G. (2009). Cytoplasmic functions of the tumour suppressor p53. Nature *458*, 1127–1130.

Havre, P.A., Abe, M., Urasaki, Y., Ohnuma, K., Morimoto, C., and Dang, N.H. (2008). The role of CD26/dipeptidyl peptidase IV in cancer. Front. Biosci. *13*, 1634–1645.

Hou, W., Xie, Y., Song, X., Sun, X., Lotze, M.T., Zeh, H.J., 3rd, Kang, R., and Tang, D. (2016). Autophagy promotes ferroptosis by degradation of ferritin. Autophagy *12*, 1425–1428.

Huerta, S., Goulet, E.J., and Livingston, E.H. (2006). Colon cancer and apoptosis. Am. J. Surg. *191*, 517–526.

Humpton, T.J., and Vousden, K.H. (2016). Regulation of cellular metabolism and hypoxia by p53. Cold Spring Harb. Perspect. Med. *6*, a026146.

Jackson, E.K. (2017). Context-dependent effects of dipeptidyl peptidase 4 inhibitors. Curr. Opin. Nephrol. Hypertens. *26*, 83–90.

Jennis, M., Kung, C.P., Basu, S., Budina-Kolomets, A., Leu, J.I., Khaku, S., Scott, J.P., Cai, K.Q., Campbell, M.R., Porter, D.K., et al. (2016). An African-specific polymorphism in the TP53 gene impairs p53 tumor suppressor function in a mouse model. Genes Dev. *30*, 918–930.

Jiang, L., Kon, N., Li, T., Wang, S.J., Su, T., Hibshoosh, H., Baer, R., and Gu, W. (2015). Ferroptosis as a p53-mediated activity during tumour suppression. Nature *520*, 57–62.

Kagan, V.E., Mao, G., Qu, F., Angeli, J.P., Doll, S., Croix, C.S., Dar, H.H., Liu, B., Tyurin, V.A., Ritov, V.B., et al. (2017). Oxidized arachidonic and adrenic PEs navigate cells to ferroptosis. Nat. Chem. Biol. *13*, 81–90.

Khoo, K.H., Verma, C.S., and Lane, D.P. (2014). Drugging the p53 pathway: understanding the route to clinical efficacy. Nat. Rev. Drug Discov. *13*, 217–236.

Lam, C.S., Cheung, A.H., Wong, S.K., Wan, T.M., Ng, L., Chow, A.K., Cheng, N.S., Pak, R.C., Li, H.S., Man, J.H., et al. (2014). Prognostic significance of CD26 in patients with colorectal cancer. PLoS ONE *9*, e98582.

Li, T., Kon, N., Jiang, L., Tan, M., Ludwig, T., Zhao, Y., Baer, R., and Gu, W. (2012). Tumor suppression in the absence of p53-mediated cell-cycle arrest, apoptosis, and senescence. Cell *149*, 1269–1283.

Linkermann, A., Skouta, R., Himmerkus, N., Mulay, S.R., Dewitz, C., De Zen, F., Prokai, A., Zuchtriegel, G., Krombach, F., Welz, P.S., et al. (2014). Synchronized renal tubular cell death involves ferroptosis. Proc. Natl. Acad. Sci. USA *111*, 16836–16841.

Liu, L., Omar, B., Marchetti, P., and Ahrén, B. (2014). Dipeptidyl peptidase-4 (DPP-4): Localization and activity in human and rodent islets. Biochem. Biophys. Res. Commun. *453*, 398–404.

Louandre, C., Ezzoukhry, Z., Godin, C., Barbare, J.C., Maziere, J.C., Chauffert, B., and Galmiche, A. (2013). Iron-dependent cell death of hepatocellular carcinoma cells exposed to sorafenib. Int. J. Cancer *133*, 1732–1742.

Louandre, C., Marcq, I., Bouhlal, H., Lachaier, E., Godin, C., Saidak, Z., François, C., Chatelain, D., Debuysscher, V., Barbare, J.C., et al. (2015). The retinoblastoma (Rb) protein regulates ferroptosis induced by sorafenib in human hepatocellular carcinoma cells. Cancer Lett. *356* (*2 Pt B*), 971–977.

Masaki, H., Okano, Y., Ochiai, Y., Obayashi, K., Akamatsu, H., and Sakurai, H. (2002). alpha-tocopherol increases the intracellular glutathione level in HaCaT keratinocytes. Free Radic. Res. *36*, 705–709.

Matsushita, M., Freigang, S., Schneider, C., Conrad, M., Bornkamm, G.W., and Kopf, M. (2015). T cell lipid peroxidation induces ferroptosis and prevents immunity to infection. J. Exp. Med. *212*, 555–568.

Muller, P.A., and Vousden, K.H. (2013). p53 mutations in cancer. Nat. Cell Biol. *15*, 2–8.

Ou, Y., Wang, S.J., Li, D., Chu, B., and Gu, W. (2016). Activation of SAT1 engages polyamine metabolism with p53-mediated ferroptotic responses. Proc. Natl. Acad. Sci. USA *113*, E6806–E6812.

Pang, R., Law, W.L., Chu, A.C., Poon, J.T., Lam, C.S., Chow, A.K., Ng, L., Cheung, L.W., Lan, X.R., Lan, H.Y., et al. (2010). A subpopulation of CD26+ cancer stem cells with metastatic capacity in human colorectal cancer. Cell Stem Cell *6*, 603–615.

Parrales, A., and Iwakuma, T. (2016). p53 as a regulator of lipid metabolism in cancer. Int. J. Mol. Sci. *17*, E2074.

Puzio-Kuter, A.M. (2011). The role of p53 in metabolic regulation. Genes Cancer *2*, 385–391.

Ren, D., Villeneuve, N.F., Jiang, T., Wu, T., Lau, A., Toppin, H.A., and Zhang, D.D. (2011). Brusatol enhances the efficacy of chemotherapy by inhibiting the Nrf2-mediated defense mechanism. Proc. Natl. Acad. Sci. USA *108*, 1433–1438.

Schott, C., Graab, U., Cuvelier, N., Hahn, H., and Fulda, S. (2015). Oncogenic RAS mutants confer resistance of RMS13 rhabdomyosarcoma cells to oxidative stress-induced ferroptotic cell death. Front. Oncol. *5*, 131.

Shimada, K., Skouta, R., Kaplan, A., Yang, W.S., Hayano, M., Dixon, S.J., Brown, L.M., Valenzuela, C.A., Wolpaw, A.J., and Stockwell, B.R. (2016). Global survey of cell death mechanisms reveals metabolic regulation of ferroptosis. Nat. Chem. Biol. *12*, 497–503.

Skouta, R., Dixon, S.J., Wang, J., Dunn, D.E., Orman, M., Shimada, K., Rosenberg, P.A., Lo, D.C., Weinberg, J.M., Linkermann, A., and Stockwell, B.R. (2014). Ferrostatins inhibit oxidative lipid damage and cell death in diverse disease models. J. Am. Chem. Soc. *136*, 4551–4556.

Sun, X., Niu, X., Chen, R., He, W., Chen, D., Kang, R., and Tang, D. (2016a). Metallothionein-1G facilitates sorafenib resistance through inhibition of ferroptosis. Hepatology *64*, 488–500.

Sun, X., Ou, Z., Chen, R., Niu, X., Chen, D., Kang, R., and Tang, D. (2016b). Activation of the p62-Keap1-NRF2 pathway protects against ferroptosis in hepatocellular carcinoma cells. Hepatology *63*, 173–184.

Tanaka, T., Camerini, D., Seed, B., Torimoto, Y., Dang, N.H., Kameoka, J., Dahlberg, H.N., Schlossman, S.F., and Morimoto, C. (1992). Cloning and functional expression of the T cell activation antigen CD26. J. Immunol. *149*, 481–486.

Thomasova, D., Bruns, H.A., Kretschmer, V., Ebrahim, M., Romoli, S., Liapis, H., Kotb, A.M., Endlich, N., and Anders, H.J. (2015). Murine double minute-2 prevents p53-overactivation-related cell death (podoptosis) of podocytes. J. Am. Soc. Nephrol. *26*, 1513–1523.

Turk, B., and Stoka, V. (2007). Protease signalling in cell death: caspases versus cysteine cathepsins. FEBS Lett. *581*, 2761–2767.

Vousden, K.H., and Ryan, K.M. (2009). p53 and metabolism. Nat. Rev. Cancer *9*, 691–700.

Wang, H., Liu, X., Long, M., Huang, Y., Zhang, L., Zhang, R., Zheng, Y., Liao, X., Wang, Y., Liao, Q., et al. (2016a). NRF2 activation by antioxidant antidiabetic agents accelerates tumor metastasis. Sci. Transl. Med. *8*, 334ra351.

Wang, S.J., Li, D., Ou, Y., Jiang, L., Chen, Y., Zhao, Y., and Gu, W. (2016b). Acetylation is crucial for p53-mediated ferroptosis and tumor suppression. Cell Rep. *17*, 366–373.

Xie, Y., Hou, W., Song, X., Yu, Y., Huang, J., Sun, X., Kang, R., and Tang, D. (2016). Ferroptosis: process and function. Cell Death Differ. *23*, 369–379.

Yamada, K., Hayashi, M., Madokoro, H., Nishida, H., Du, W., Ohnuma, K., Sakamoto, M., Morimoto, C., and Yamada, T. (2013). Nuclear localization of CD26 induced by a humanized monoclonal antibody inhibits tumor cell growth by modulating of POLR2A transcription. PLoS ONE *8*, e62304.

Yang, W.S., and Stockwell, B.R. (2016). Ferroptosis: death by lipid peroxidation. Trends Cell Biol. *26*, 165–176.

Yang, W.S., SriRamaratnam, R., Welsch, M.E., Shimada, K., Skouta, R., Viswanathan, V.S., Cheah, J.H., Clemons, P.A., Shamji, A.F., Clish, C.B., et al. (2014). Regulation of ferroptotic cancer cell death by GPX4. Cell *156*, 317–331.

Yu, Y., Xie, Y., Cao, L., Yang, L., Yang, M., Lotze, M.T., Zeh, H.J., Kang, R., and Tang, D. (2015). The ferroptosis inducer erastin enhances sensitivity of acute myeloid leukemia cells to chemotherapeutic agents. Mol. Cell. Oncol. *2*, e1054549.

Yuan, H., Li, X., Zhang, X., Kang, R., and Tang, D. (2016). Identification of ACSL4 as a biomarker and contributor of ferroptosis. Biochem. Biophys. Res. Commun. *478*, 1338–1343.

Zhong, J., Rao, X., and Rajagopalan, S. (2013). An emerging role of dipeptidyl peptidase 4 (DPP4) beyond glucose control: potential implications in cardiovascular disease. Atherosclerosis *226*, 305–314.

Zhu, S., Zhang, Q., Sun, X., Zeh, H.J., 3rd, Lotze, M.T., Kang, R., and Tang, D. (2017). HSPA5 regulates ferroptotic cell death in cancer cells. Cancer Res. *77*, 2064–2077.